Estimate of ULF electromagnetic noise caused by a fluid flow during seismic or volcano activity

Vadim V. Surkov[1,*], Vyacheslav A. Pilipenko[2]

[1] *National Research Nuclear University MEPhI, Moscow, Russia*

[2] *Institute of Physics of the Earth, Russian Academy of Science, Moscow, Russia*

ABSTRACT

The elaboration of theoretical models, even oversimplified, capable to estimate an expected electromagnetic effect during earthquake preparation process is not less important than the advancement of observational technique to detect seismic-related electromagnetic perturbations. Here possible mechanisms of ULF electromagnetic noise associated with seismic or volcanic activity are discussed. The electrokinetic (EK) and magneto-hydrodynamic (MHD) effects due to an irregular flow of conducting rock fluid or magma flow are being revised. The conventional theory of EK effect in a water-saturated rock has been advanced by consideration of elliptic-shaped channels. A contribution of both mechanisms to observed ULF signal on the ground is shown to be dependent on the pore channel size/rock permeability. Estimates of magnetic and electrotelluric perturbations caused by magma motion along a volcano throat indicate on the important role of the surrounding rock conductivity. These estimates have proven that the mechanisms under consideration are able to generate ULF electromagnetic perturbations which could be detected by modern magnetometers under favorable conditions.

1. Introduction

At the time being it is clear that the tectonic plate dynamics can provide long-term (tens-hundred years) earthquake prediction, but not short-term (days-weeks) seismic warning. This situation demands the search for alternative techniques for the short-term prediction of impending earthquakes. A special credit has been paid in the last decades to the study of a variety of electromagnetic and other non-seismic phenomena possibly associated with the earthquake preparation process. Considerable efforts have been devoted to the study of electromagnetic signals/noise in the Ultra-Low-Frequency (from few mHz to tens of Hz) band (extensive list of references can be found in papers collected by Hayakawa and Molchanov [2002], Molchanov and Hayakawa [2008], and Hayakawa [2013]). These studies were stimulated by effective detection of electro-magnetic effects in a wide frequency band accompanying sample fracture in laboratory [e.g., Cress et al. 1987, Freund 2000, Vallianatos et al. 2012]. Easy availability of data from world-wide array (~200) of magnetometers favored an extensive search for seismic-related ULF anomalies. However, it was soon realized that ULF perturbations possibly related to the seismic activity are weak as compared with typical magnetosphere/ionosphere pulsations and industrial interference, so they can be directly recorded only under exceptionally favorable conditions: close proximity to an epicenter of impending earthquake and geomagnetically quiet period [e.g., Molchanov et al. 1992]. Therefore, much effort has been concentrated in search of peculiar features of seismic-related ULF perturbations that would make possible to reveal them even under low signal/noise ratio. There were numerous attempts to find anomalous ULF behavior with a simple measure of their spectral features - the slope of averaged power spectrum ("fractal properties") [e.g., Gotoh et al. 2004]. Another approach uses the ratio between the ULF vertical Z and horizontal G components. It is expected that an underground source produces a signal on the ground with larger Z/G ratio than a magnetospheric/ionospheric source does [Hayakawa et al. 1996]. Attempts to discriminate seismic and magnetospheric ULF sources were made with the use of the gradient observations [Krylov and Nikiforova 1995, Kopytenko et al. 2006]. More advanced technique - the principal component analysis, seems promising to identify and suppress magnetospheric pulsations and industrial interference [Gotoh et al. 2002]. However, many of seemingly successful results of seismic-related ULF perturbation discovery could not pass simple tests: lack of correlation with geomagnetic activity and absence of claimed features at distant stations [Campbell 2009, Thomas et al. 2009, Masci 2011].

Development in a contentious field of earthquake prediction requires an advance not only in monitoring technique, but in a reliable estimate of physical models plausibility. Electromagnetic disturbances in the ULF frequency band, with the skin-depth corresponding to crustal earthquake hypocentral depth, are still considered as one of the most promising monitors of earthquake precursors. Majority of modern theories predict that the amplitude of the seismic-related ULF signals can be of the order of or greater than background ULF noise at the epicentral distances no more than one hundred km. The generation mechanisms of seismic-related ULF electromagnetic fields considered so far (see the book by Surkov and Hayakawa [2014] for a complete review) comprise:

- the electric charge redistribution during microcracking [Molchanov and Hayakawa 1995]. However, the estimated amplitude of this effect seems to be much lower than the background noise level because of the random orientation of the dipole moments of individual microcracks [Surkov and Hayakawa 2014];

- inductive geomagnetic response to the tension crack openings in a conductive rock [Surkov 1997, Surkov and Hayakawa 2006]. An advantage of this mechanism is that the effective magnetic moments of all cracks are co-directed and anti-parallel to the Earth magnetic field; therefore they operate as a coherent amplifier of ULF noise;

- the stress-induced electric current in the rock caused by the changes in mobility of charged dislocations [Tzanis and Vallianatos 2002] and/or point defects [Freund 2000].

Some theories interpreted the occurrence of ULF electromagnetic noise as a result of the crust fluid dynamics. The flow of high-pressure fluid in fault zones has an irregular character ("stop-and-start") [Byerlee 1993]. Such non-steady filtration of conductive fluid is to be accompanied by electromagnetic disturbances due to magnetohydrodynamic (MHD) effect [Draganov et al. 1991]. However, the importance of this mechanism was overestimated by four orders of magnitude by Draganov et al. [1991] because of an unrealistic rock permeability used in this study [Surkov and Pilipenko 1997, 1999].

The electrokinetic effect (EK) is another promising candidate which can give a plausible interpretation of anomalous ULF electromagnetic disturbances observed before strong earthquakes [e.g., Pride 1994]. The EK effect was applied to interpret both the occurrence of precursory ULF perturbation before earthquake [Ishido and Mizutani 1981, Surkov et al. 2002] and a co-seismic electric impulse caused by propagating seismic waves [Nagao et al. 2000]. In realistic geophysical media

a combination of several mechano-electromagnetic mechanisms may occur: for example, a high level of geoacoustic impulses produced by microcracking can enhance the fluid filtration and EK processes [Pilipenko and Fedorov 2014].

Similar ULF electromagnetic effects may accompany volcano activity [Johnston 1989, Uyeda et al. 2002]. Numerous underground chambers in the rock surrounding a volcano are filled with underground fluid whose pressure varies from hydrostatic level up to lithostatic pressure depending on the chamber sizes, rock permeability, and other parameters. The magma movement along the volcano throat and variations of tectonic stresses may cause the destruction of chambers followed by changes in pore fluid pressure, which in turn results in generation of EK currents [Johnston 1997, Zlotnicki and Nishida 2003]. Indeed, several days before and after a volcano eruption electromagnetic noise in the band 0.01-0.6 Hz was observed by Fujinawa et al. [1992]. At the same time, an irregular movement of a highly-conductive magma along a volcano throat can produce magnetic ULF noise by the MHD effect [Kopytenko and Nikitina 2004a, 2004b].

To evaluate the significance of possible effects and their dependence on crust parameters and to identify favorable locations for electromagnetic monitoring one needs an approximate but handy model. Hopefully, on the basis of adequate theoretical models a special technique, but not standard magnetometers, for a search of seismic-related ULF perturbations will be designed. Therefore, the development of analytical models, though sometimes oversimplified, is of primary importance for the progress in search of reliable ULF electromagnetic precursors. In this paper we revisit the conventional theory of the EK phenomenon by incorporating of the MHD effect in the description of pore fluid flow. Then we compare contribution of the EK and MHD mechanisms for various sizes and shapes of pores/channel cross sections. We model pores/cracks as ellipsoidal channels and apply this model for a qualitative estimate of ULF magnetic perturbations caused by seismic or volcano activity.

2. The electrokinetic effect in a medium with elliptic-shaped channels

The EK effect in multiphase porous media builds up as a result of fluid filtration followed by appearance of a contact potential drop at the interfaces. It is usually the case that the groundwater contains the electrolyte solutions including ions and dissociated molecules. The surfaces of cracks and pores can adsorb ions of certain polarity from the solution that results in a charge separation between the crack walls and fluid followed by

the formation of electric double layer (EDL) at the solid-fluid interface. As a rule, the solid is negatively charged due to the adsorption of hydroxyl groups originating from acid dissociation [Parks 1965]. The EDL includes a diffuse mobile layer extending into the fluid phase. The moving fluid drags solvated cations thereby exciting the EK current.

We introduce the model of a pore as a cylindrical channel with the elliptic cross-section $x^2/a^2 + y^2/b^2 = 1$, where a and b are the ellipse semi-axes. In this approach, we can analyze the effect of the cross-section shape on the EK phenomenon since this model involves either circular channels ($a = b$) or plane cracks ($a \gg b$). A viscous fluid is assumed to flow along z axis. The channel is surrounded by an incompressible solid matrix. The crust is immersed in the geomagnetic field $\mathbf{B}$. We assume a laminar fluid flow because of small value of Reynolds number [Sparnaay 1972]. The fluid velocity $\mathbf{V}$ is controlled by the fluid pressure gradient ∇P along a channel, so the velocity distribution over the channel cross-section $\mathbf{V}(x,y)$ is given by [Landau and Lifshitz 1959]

$$\mathbf{V} = -\frac{a^2 b^2}{2\eta (a^2 + b^2)} \left(1 - \frac{x^2}{a^2} - \frac{y^2}{b^2}\right) \nabla P \qquad (1)$$

where η is the fluid viscosity. Due to the EK effect the fluid contains an excess of ions, more frequently cations, while the channel wall adsorbs the opposite electric charges. As a result, the EDL is formed in the fluid near the channel walls. The typical size of the EDL is of the order of cation Debye radius which is much smaller than the characteristic size of the channel [Sparnaay 1972]. The electric potential φ in the pore fluid satisfies the Poisson equation

$$\nabla^2 \varphi = -\frac{q \Delta n}{\varepsilon \varepsilon_0} \qquad (2)$$

where q denotes the cation charge, Δn is the number density of the cation excess, ε is the dielectric permeability of the fluid, and ε_0 is the dielectric permittivity of a free space. The total current density inside the channel is composed from the conduction and Hall currents, and the EK current with density $\mathbf{j}_{EK} = q \Delta n \mathbf{V}$, as follows:

$$\mathbf{j} = \sigma_f (\mathbf{E} + \mathbf{V} \times \mathbf{B}) + \mathbf{j}_{EK} \qquad (3)$$

Here σ_f is the fluid conductivity, and $\mathbf{E} = -\nabla \varphi$ is the electric field strength. It is generally accepted that the conduction current $\sigma_f \mathbf{E}$ is much larger than the Hall current $\sigma_f (\mathbf{V} \times \mathbf{B})$. The mean density of the EK

current $\langle \mathbf{j}_{EK} \rangle$, averaged over the channel cross-section, is determined from (2) through the following integral

$$\langle \mathbf{j}_{EK} \rangle = \frac{1}{S} \int_S \mathbf{j}_{EK} dS = -\frac{\varepsilon \varepsilon_0}{\pi ab} \int_S \nabla^2 \varphi \mathbf{V} dS. \qquad (4)$$

where $S = \pi ab$ is the area of the cross-section and dS is the small element of this area. Further, for the sake of simplicity we shall omit the symbol $\langle \ \rangle$.

Substituting Equation (1) for $\mathbf{V}$ into Equation (4) and taking into account the fact that φ changes rapidly in the narrow EDL near the channel walls, one can simplify the integral in Equation (4). In the case of a circular cross-section ($a = b$), Equation (4) is reduced to the known form [e.g., Surkov et al. 2002]

$$\langle \mathbf{j}_{EK} \rangle = -\frac{\varepsilon \varepsilon_0 \zeta}{\eta} \nabla P \qquad (5)$$

Here ζ is the potential drop across the EDL, or so-called zeta potential.

In the case of an elliptic cross-section some mathematical complications can arise due to the potential variations on the surface of channel. This problem is studied in a greater detail in the Appendix. The analysis shows that if the potential is assumed to be constant on the channel surface then the EK current density is given by the same Equation (5). Thus, in the first approximation the EK currents through the circular and elliptic cross-sections are described by the same equation. Owing to a finite conductivity σ_r of the dry rock surrounding the channel the surface potential tends to be equal. The above approach holds true if the relaxation time $\propto \varepsilon_0 / \sigma_r$ is much smaller than the period of variations of pore fluid pressure and velocity, and this requirement is valid in the processes under consideration.

In any homogeneous conducting medium with an arbitrary distribution of pore fluid pressure, the total magnetic effect due to EK effect vanishes [Fitterman 1979]. That is, on average the magnetic effect of the electric current resulted from the motion of the pore fluid is cancelled by the effect of the backward conduction current. A non-zero magnetic effect occurs only in an inhomogeneous medium, and its magnitude depends on the degree of heterogeneity.

3. MHD effect and the Onsager reciprocal relations

In this section we ignore the EK effect for a moment and focus on the MHD effect only. The motion of the conducting underground fluid in the geomagnetic field $\mathbf{B}$ gives rise to the generation of Hall current $\mathbf{j}_H = \sigma_f (\mathbf{V} \times \mathbf{B})$ pointed normal to the channel axis. Taking into account Equation (1) for $\mathbf{V}$ we obtain

$$\mathbf{j}_H = -\frac{\sigma_f a^2 b^2}{2\eta\left(a^2+b^2\right)}\left(1-\frac{x^2}{a^2}-\frac{y^2}{b^2}\right)(\nabla P \times \mathbf{B}) \qquad (6)$$

In the case of non-conductive rock the Hall current is closed by the conduction and EK currents in the fluid. In fact, the total current may flow out of the channel due to a finite rock conductivity. The closed system of longitudinal and transverse electric currents excited in the rock and fluid is shown in Figure 1.

According to De Groot and Mazur [1962], the mean EK current density in rocks reads $\langle \mathbf{j}_{EK}\rangle = -L_{EV}\nabla P$, where L_{EV} stands for the streaming current coupling coefficient. This coefficient can be derived from (4) to yield $L_{EV} = -\varepsilon\varepsilon_0\zeta m/(\eta\beta^2)$, where m is the rock porosity, and β is the pore space tortuosity. Similarly, generalizing (6) for the Hall current density yields, $\langle \mathbf{j}_H\rangle = -L_{EB}(\nabla P \times \mathbf{B})$, where $L_{EB} \sim L_{EV}\sigma_f S/(4\pi\varepsilon\varepsilon_0\zeta) = \sigma_f mS/4\pi\eta\beta^2$ is the Hall coefficient. In a more complete theory the relationship between L_{EB} and L_{EV} should depend on the rock permeability rather than on S. Thus the total mean current density in a porous rock can be written as follows:

$$\mathbf{j} = -\Sigma\nabla\varphi - L_{EV}\nabla P - L_{EB}(\nabla P \times \mathbf{B}) \qquad (7)$$

where $\Sigma = L_{EE}$ stands for the mean rock conductivity.

To summarize, we note that the electric current in porous rocks can result in electroosmotic and other kinetic effects. According to the Onsager reciprocal relations the mean flux density of the fluid flow, $\mathbf{J}$, is given by

$$\mathbf{J} = -L_{VE}\nabla\varphi - L_{VV}\nabla P - L_{BE}(\nabla P \times \mathbf{B}) \qquad (8)$$

where $L_{EV} = L_{VE}$, and $L_{EB} = -L_{BE}$. The first term in the right-hand part of Equation (8) describes the electroosmotic effect, the second term describes Darcy law in a porous rock, while the last term arises from the magnetic force acting on a moving conductive fluid. The Equations (7) and (8) permit the extension of basic thermodynamic principles [e.g., De Groot and Mazur 1962] to the case of rock immersed in ambient magnetic field.

In order to compare the EK and Hall current densities, we return to the consideration of individual channels. Combining Equations (5) and (6), assuming $a \sim b$ and taking into account that the Hall current reaches its peak value at the center of the channel, yields

$$\frac{j_H}{j_{EK}} \sim \frac{SB\sigma_f\sin\alpha}{4\pi\varepsilon\varepsilon_0\zeta} \qquad (9)$$

where α is the angle between vectors ∇P and $\mathbf{B}$. Notice that if $b \ll a$; that is, in the case of plane channel/crack,
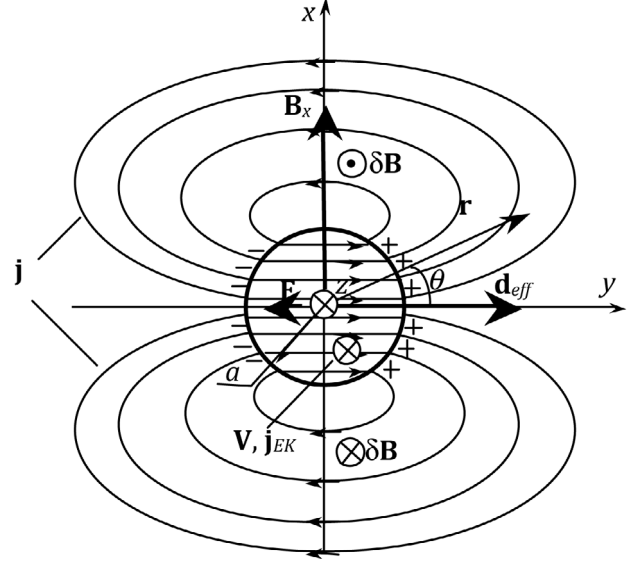
Figure 1. A geometry of the magma flow model and schematic configuration of total currents $\mathbf{j}$ flowing across a volcano throat. The magma velocity $\mathbf{V}$ is directed along z axis. The effective current moment $\mathbf{d}_{eff}$ is perpendicular to $\mathbf{V}$ and geomagnetic field $\mathbf{B}$. Circles with dots and crosses indicate the directions of magnetic disturbance $\delta\mathbf{B}$ and magma velocity.

the above ratio includes the additional small factor $b/a \ll 1$.

It follows from Equation (9) that the EK current dominates over the Hall one in narrow channels; that is, under the requirement

$$S \ll S_* = \frac{4\pi\varepsilon\varepsilon_0\zeta}{\sigma_f B\sin\alpha} \qquad (10)$$

Taking the typical values of the groundwater parameters $\zeta = 10 - 50$ mV [Ishido and Mizutani 1981], $\varepsilon = 80$, the electrolyte solution conductivity $\sigma_f = 0.1 - 0.2$ S/m, geomagnetic field $B = 5\times10^{-5}$ T and $\alpha = \pi/3$, we obtain the following estimate of the critical cross-section $S_* \approx 0.1 - 1$ m^2. It should be emphasized that this is only a rough estimation since the pore fluid may acquire other properties under the influence of high stress and temperature deep in the crust.

Equation (10) shows that the Hall current appears to have insignificant effect in natural rocks because of small sizes of pores and channels. However, it seems likely that the MHD effects can be significant in the broken rock with high pore space and in the case of macroscopic fluid flow such as magma motion along a volcano throat.

4. Geomagnetic perturbations due to magma motion in a volcano throat

ULF electromagnetic noise occasionally observed during volcano pre-eruption activity is assumed to be due to the motion of a conducting magma along the

throat. The oscillations of the magma surface in volcano cavity, vortical motion due to Coriolis force, as well as upward magma lifting along the volcano throat can serve as possible mechanisms for ULF electromagnetic noise [Kopytenko and Nikitina 2004a, 2004b].

Here we estimate the effect caused by magma lifting. In order to build an analytically treatable model, we assume that the magma is confined within an ellipsoidal underground cavity. The origin of the coordinate system is in the center of the ellipsoid and the coordinate axes coincide with axis of ellipsoid symmetry in such a way that the ellipsoid surface is described by the following equation $x^2/a^2 + y^2/b^2 + z^2/c^2 = 1$, where a, b and c are the ellipsoid semi-axes. This model is a convenient mathematical approximation because in subsequent study parameter c will tend to infinity in order to describe the magma motion along the infinite cylindrical channel. The cross-section of this cylinder is assumed to be greater than the critical value S_* in Equation (10). This implies that the EK in Equation (3) can be ignored. In this notation the movement of conductive magma with velocity $\mathbf{V}$ in the geomagnetic field $\mathbf{B}$ results in the generation of electric current with density $\mathbf{j} = \sigma_m(\mathbf{E} + \mathbf{V} \times \mathbf{B})$, where σ_m is the magma conductivity. At the same time, in the surrounding crust the conduction back current $\mathbf{j} = \sigma_r \mathbf{E}$ flows. Usually, the rock conductivity $\sigma_r = 10^{-3} - 10^{-2}$ S/m is much smaller than that of magma $\sigma_m = 10^{-2} - 10$ S/m [Gaillard and Marziano 2005].

In the ULF frequency range, the electromagnetic fields and currents may be considered as quasi-stationary. For mathematical simplicity we suppose that fluid velocity $\mathbf{V}$ is steady and directed along z axis. Further we shall apply this approach to an infinite cylinder ($c \rightarrow \infty$) where such kind of fluid motion is possible. The problem under consideration is mathematically similar to the known problem of polarization/magnetization of an ellipsoid in a homogeneous electric/magnetic field [Landau and Lifshitz 1960]. Based on this similarity, one can find that electromagnetic perturbation outside the ellipsoid is derived via its effective current moment

$$\mathbf{d}_{eff} = \frac{\sigma_r M_x \hat{\mathbf{x}}}{\sigma_m n^{(x)} + \sigma_r \left(1 - n^{(x)}\right)} + \frac{\sigma_r M_y \hat{\mathbf{y}}}{\sigma_m n^{(y)} + \sigma_r \left(1 - n^{(y)}\right)} \qquad (11)$$

Here M_x and M_y are the components of the Hall current moment $\mathbf{M} = \mathbf{j}_H W$, $\hat{\mathbf{x}}$ and $\hat{\mathbf{y}}$ stands for unit vectors, and $W = 4\pi abc/3$ is the ellipsoid volume. The depolarization factors $n^{(x)}$ and $n^{(y)}$ depend on parameters a, b, c. Notice that the vectors $\mathbf{d}$ and $\mathbf{M}$ are not parallel.

Now we consider a case when the conductive magma flows along an infinite cylinder/throat with a fixed radius a. This geometry corresponds to parameters of the ellipsoid as follows: $a = b$ and $\tilde{c} \rightarrow \infty$. For this case one gets $n^{(x)} = n^{(y)} = 0.5$ [Landau and Lifshitz 1960]. Substituting these parameters into Equation (11), we come to the relationship for the effective current moment $\mathbf{d}_{eff}$ per unit of the cylinder length

$$\mathbf{d}_{eff} = \frac{\mathbf{d}}{c} = \frac{2\pi a^2 \sigma_m \sigma_r}{\sigma_m + \sigma_r} (\mathbf{V} \times \mathbf{B}) \qquad (12)$$

Let axis y be parallel to the vector $\mathbf{d}_{eff}$ as shown in Figure 1, so the vectors $\mathbf{V}$ and $\mathbf{B}$ are in the plane x, z.

Due to the Hall current $\mathbf{j}_H = \sigma_m(\mathbf{V} \times \mathbf{B})$ the cylinder is polarized in such a way that the opposite charges accumulate at the cylinder surface as schematically shown in Figure 1. The same figure shows the transverse electric field $\mathbf{E}$ which is parallel to the conduction current $\mathbf{j}_c = \sigma_m \mathbf{E}$, flowing opposite to the Hall current. The total current $\mathbf{j} = \mathbf{j}_H + \mathbf{j}_c$ is closed by the conduction currents, $\mathbf{j} = \sigma_r \mathbf{E}$, in the surrounding rocks. The system of currents flowing across the channel is schematically shown in Figure 1. This current system generates magnetic disturbance $\delta\mathbf{B}$ along the cylinder z-axis.

The problem under consideration is axially symmetric, therefore we may introduce the polar coordinates (r, θ): r is the distance from channel axis and θ is the angle measured from positive x-axis direction. The component of magnetic disturbance along z axis is derived via the effective moment (12) as follows:

$$\delta B_z = -\frac{\mu_0 d_{eff} \cos\theta}{2\pi a} \begin{cases} r/a & (r < a) \\ a/r & (r > a) \end{cases} \qquad (13)$$

Combining (12) and (13), we obtain the magnetic perturbations in the region outside the cylinder ($r > a$):

$$\delta B_z = -\frac{\mu_0 a^2 \sigma_m \sigma_r V B_x \cos\theta}{r(\sigma_m + \sigma_r)}, \qquad (14)$$

where B_x is the geomagnetic field component along x-axis. The magnetic disturbance decays away from the cylinder axis as $\propto r^{-1}$.

If the magma conductivity is much greater than the rock conductivity, that is $\sigma_m \gg \sigma_r$, then the relationship (14) can be simplified

$$\delta B_z = -\frac{\mu_0 a^2 \sigma_r V B_x \cos\theta}{r} \qquad (15)$$

Equation (15) differs from the relationship derived by Kopytenko and Nikitina [2004a, 2004b] by a small factor $\sigma_r/\sigma_m \ll 1$. This difference is due to the fact that they ignored the conductivity of the crust σ_r and thus

overestimated an expected magnitude of magnetic perturbations. The rock conductivity determines the current leakage from a channel into the environment, and thus may greatly affect the magnitude of magnetic perturbations.

The transverse conduction current inside magma is directed opposite to the Hall current thereby reducing it. As a result, the total current inside the cylinder is smaller than j_H and is directed opposite to the electric field $\mathbf{E}$:

$$\mathbf{j} = \frac{\sigma_r}{\sigma_m + \sigma_r}\mathbf{j}_H, \quad \mathbf{E} = -\frac{\mathbf{j}_H}{\sigma_m + \sigma_r} \qquad (16)$$

It should be noted that both $\mathbf{j}$ and $\mathbf{E}$ are homogeneous inside the cylinder (see Figure 1).

The electric field induced in the surrounding rock due to the magma movement in the geomagnetic field is estimated to be

$$E_r = \frac{|\mathbf{j}_H|a^2\sin\theta}{(\sigma_m + \sigma_r)r^2}, \quad E_\theta = -E_r\mathrm{ctg}\theta \qquad (17)$$

If $\sigma_m \gg \sigma_r$, this field only weakly depends on the rock conductivity. The electric field disturbance decays away from the cylinder more rapidly $\propto r^{-2}$ than the magnetic disturbance does.

A typical amplitude of magnetic disturbance estimated from relationship (15) is as follows: $\delta B_{max} \sim \mu_0 a^2 \sigma_r V_{max} B/r$, where V_{max} is the amplitude of the magma flow velocity variations. For the same parameters $\sigma_r = 10^{-3} - 10^{-2}$ S/m, $B = 5 \cdot 10^{-5}$ T, $V_{max} = 5$ m/s, $a = 0,1 - 1$ km as used by Kopytenko and Nikitina [2004a, 2004b] one gets the estimate of magnetic disturbance at distance $r = 1$ km of $\delta B_{max} \sim 3 \cdot 10^{-3} - 3$ nT. This estimate is compatible with observations of the magnetic perturbation, about several nT, during volcano activity [Johnston 1997]. The electric component of disturbance estimated from (17) is as follows: $E_{max} \sim a^2 V_{max} B/r^2$. For the same parameters $E_{max} \sim 2.5 - 250$ μV/m. Telluric fields of such amplitude can be detected by modern sensors.

The apparent impedance of disturbance produced by the magma flow dynamics can be estimated as $Z = \mu_0 \delta E/\delta B \sim (\sigma_r r)^{-1}$. This value differs considerably from the apparent impedance of magnetospheric waves, and this distinction could be used for their discrimination.

The spectrum of the ULF electromagnetic noise observed on the ground is determined by a source spectrum and by attenuation factor due to the skin-effect. The fluctuations of magma velocity along with oscillations of the magma surface or seismic vibrations of the underground cavity can contribute to the source spectrum. Fundamental frequency of such vibrations is $f \sim V_S/l$, where $l = 0.1 - 10$ km is the cavity scale, and $V_S = 2 - 2.5$ km/s is the magma sound velocity. For these typical values, this frequency, $f \sim 0.2 - 25$ Hz, falls into ULF/ELF band which is consistent with observations [Fujinawa et al. 1992, Johnston 1997].

The analytical relationships (14) and (15) show that magnetic perturbation depends mainly on the conductivity of the surrounding rocks rather than on magma conductivity. Under low rock conductivity, the generated system of Hall currents is nearly completely short-circuited by the conductivity currents within magma, and the magnetic effect on the ground is to be weak. Under high rock conductivity the conduction currents expand far into the rock, and the magnetic effect on the ground is more significant.

5. Discussion

The fact that some published results on ULF "precursors" were not supported upon a more detailed analysis [Thomas et al. 2009, Masci 2011] should not rule out the problem of seismo-electromagnetic phenomena entirely. For a search of seismic-related ULF signals just standard magnetic observations could be inappropriate because of a small value of signal-to-noise ratio. An elaboration of specialized detection methods of ULF seismic-related signals/noise, and their discrimination from the magnetospheric waves, are to be based on some models, even oversimplified. The elaboration of theoretical models capable to estimate an expected effect under observational conditions is not less important than the advancement of observational technique. The proposed paper is a step in this direction.

The increase of ULF electromagnetic noises associated with enhancement of seismic or volcano activity can be explained in terms of different physical mechanisms. The average current densities and fluid fluxes can be described in terms of Onsager reciprocal relations. The rough estimate of the EK and Hall current amplitudes has shown that the EK effect plays a key role as the mean cross-section of channels is smaller than a certain critical value. This situation is typical for realistic water-saturated rocks with a weak permeability. The MHD effects dominate a macroscopic flow such as the groundwater migration through a broken rock with a high permeability or magma motion along a volcano throat. In the above consideration we have neglected the atmosphere-ground interface. The account of it may modify the estimates, but not significantly, less than by factor about 2 [Fedorov et al. 2001].

Our analysis has shown that the EK and Hall currents in an individual channel have different structures.

The EK and back conduction currents are directed along the fluid flow; that is, parallel to the channel walls, whereas the Hall currents are predominantly concentrated in the cross-section of the channels. Therefore, the resulted magnetic disturbances have different field polarization. The magnetic field perturbation due to the MHD effect is parallel to the axis of a channel (δB_z component in Figure 1). By contrast, the magnetic perturbation caused by the EK effect (δB_r and δB_θ components) is perpendicular to the channel axis. The averaging of these effects over the rock volume cannot cancel this tendency since there is a predominant direction in ground fluid filtration or magma motion. However, in practice it seems very difficult to distinguish between these two factors only on the basis of signal polarizations. Actually the fluid-filled cracks, pores and channels are randomly distributed in the rock. In order to interpret the observations adequately, the Hall and EK current densities given by Equations (5) and (6) should be averaged over the rock volume. This problem requires further consideration with a numerical modeling.

It follows from our model that the EK current densities through the circular and elliptic cross-sections are described by the same equation. So, we may assume that the cross-section shape of pore channels has a minimal effect on the EK phenomena except for the case of very narrow cracks when the distance between the crack surfaces becomes comparable with the EDL thickness. The latter case should be studied separately because of the overlap of the adjacent EDLs inside the crack space. It appears that the crack tortuosity may have a more significant effect on both the rock permeability and EK effect.

Using a simplified model of steady flow of conducting magma along a cylindrical channel we have estimated the amplitude of magnetic perturbations at small distances from a volcano. In contrast to [Kopytenko and Nikitina 2004a, 2004b], we have found that the rock conductivity reduces this estimate essentially. However, the upper limit of this estimate (~3 nT and ~250 μV/m) is close to the amplitudes of signals occasionally observed during volcanic eruption and the enhanced seismic activity possibly associated with magma motion. Despite uncertainties with factual parameters of magma flows, volcano geometry, and crust parameters, the estimates prove that under favorable conditions ULF magnetic monitoring on the ground of the underground magma flow becomes feasible.

The ULF electromagnetic effects possibly associated with enhancement of seismic activity can be explained in terms of different physical mechanisms. In this study we have reanalyzed only two such mecha-

nisms - the EK and MHD effects. The ULF magnetic perturbation produced by acoustic noise in conducting layers of the ground is another promising mechanism [Surkov 1997, Surkov and Hayakawa 2006]. What mechanism makes a major contribution to the observed seismic-related signals is the key question to be answered. A progress in observational studies of possible anomalous seismic-related ULF electromagnetic fields would be impossible without elaboration of specialized detection methods, based on adequate models. Elaboration of such models may indicate what ULF signatures (e.g., polarization, impedance, gradients, waveforms, etc.) can be used as an indicator of an impending earthquake or volcano eruption.

6. Conclusions

We have considered the EK and MHD effects due to an irregular flow of the crust fluid or magma as a possible mechanism of ULF electromagnetic noise associated with seismic or volcanic activity. The conventional theory of the EK effect has been advanced by considering elliptic-shaped channels. A contribution of both mechanisms to observed magnetic disturbance is shown to be different depending on the pore/channel permeability. Magnitudes of magnetic and electric field perturbations depend on a contrast between fluid/magma and rock conductivities. The suggested model proves the possibility to estimate analytically by order of magnitude the expected electromagnetic effect of the fluid/magma flow under chosen geophysical parameters. Such estimates prove a feasibility of the ULF electromagnetic monitoring of magma dynamics in a volcano conduit, supplementary to the observations of volcano tremor.

References

Byerlee, J. (1993). Model for episodic flow of high-pressure water in fault zones before earthquakes, Geology, 21, 303-306.

Campbell, W.H. (2009). Natural magnetic disturbance fields, not precursors, preceding the Loma Prieta earthquake, J. Geophys. Res., 114, A05307; doi:10.1029/2008JA013932.

Cress, G.O., B.T. Brady and G.A. Rowell (1987). Sources of electromagnetic radiation from fracture of rock samples in the laboratory, Geophys. Res. Lett., 14, 331-334.

De Groot, S.R., and P. Mazur (1962). Non-Equilibrium Thermodynamics, North-Holland, Amsterdam; Wiley, New York.

Draganov, A.B., U.S. Inan and Yu.N. Taranenko (1991).

ULF magnetic signature at the Earth surface due to ground water flow: a possible precursor to earthquakes, Geophys. Res. Lett., 18, 1127-1130.

Fedorov, E., V. Pilipenko and S. Uyeda (2001). Electric and magnetic fields generated by electrokinetic processes in a conductive crust, Phys. Chem. Earth, 26, 793-799.

Fitterman, D.V. (1979). Theory of electrokinetic-magnetic anomalies in a faulted half-space, J. Geophys. Res., 84, 6031-6040.

Freund, F. (2000). Time-resolved study of charge generation and propagation in igneous rocks, J. Geophys. Res., 105, 11001-11019.

Fujinawa, Y., T. Kumagai and K. Takahashi (1992). A study of anomalous underground electric-field variations associated with a volcanic eruption, Geophys. Res. Lett., 19, 9-12.

Gaillard, F., and G.I. Marziano (2005). Electrical conductivity of magma in the course of crystallization controlled by their residual liquid composition, J. Geophys. Res., 10, B06204; doi:10.1029/2004JB003282.

Gotoh, K., Y. Akinaga, M. Hayakawa and M. Hattori (2002). Principal component analysis of ULF geomagnetic data for Izu islands earthquakes in July 2000, J. Atmos. Electricity, 22, 1-12.

Gotoh, K., M. Hayakawa, N.A. Smirnova and K. Hattori (2004), Fractal analysis of seismogenic ULF emissions, Phys. Chem. Earth, 29, 419-424.

Hayakawa, M., R. Kawate, O.A. Molchanov and K. Yumoto (1996). Results of ultra-low frequency magnetic field measurements during the Guam earthquake of 8 August 1993, Geophys. Res. Lett., 23, 241-244.

Hayakawa, M., and O. Molchanov, eds. (2002). Seismo Electromagnetics, TERRAPUB, Tokyo, 477 p.

Hayakawa, M., ed. (2013). Earthquake Prediction Studies: Seismo Electromagnetics, TERRAPUB, Tokyo.

Ishido, T., and H. Mizutani (1981). Experimental and theoretical basis of electrokinetic phenomena in rock-water systems and its applications to geophysics, J. Geophys. Res, 86B, 1763-1775.

Johnston, M.J.S. (1989). Review of magnetic and electric field effects near active faults and volcanoes in the USA, Phys. Earth Planet. In., 57, 47-63.

Johnston, M.J.S. (1997). Review of electric and magnetic fields accompanying seismic and volcanic activity, Surv. Geophys., 18, 441-475.

Kopytenko, Yu.A., and L.V. Nikitina (2004a). ULF oscillations in magma in the period of seismic event preparation, Phys. Chem. Earth, 29, 459-462.

Kopytenko, Yu.A., and L.V. Nikitina (2004b). A possible model for initiation of ULF oscillation in magma, Annals of Geophysics, 47, 101-105.

Kopytenko, Yu.A., V.S. Ismaguilov, K. Hattori and M.

Hayakawa (2006). Determination of hearth position of a forthcoming strong EQ using gradients and phase velocities of ULF geomagnetic disturbances, Phys. Chem. Earth, 31, 292-298.

Krylov, S.M., and N.N. Nikiforova, (1995). About ULF electromagnetic emission of active geological medium, Fizika Zemli, 6, 42-57.

Landau, L.D., and E.M. Lifshitz (1959). Fluid Mechanics (vol. 6 of A Course on Theoretical Physics), Pergamon Press, Oxford.

Landau, L.D., and E.M. Lifshitz (1960). Electrodynamics of Continuous Media (vol. 8 of A Course on Theoretical Physics), Pergamon Press, Oxford.

Masci, F. (2011). On the seismogenic increase of the ratio of the ULF geomagnetic field components, Phys. Earth Planet. In.; doi:10.1016/j.pepi.2011.05.001.

Molchanov, O.A., Yu.A. Kopytenko, P.M. Voronov, E.A. Kopytenko, T.G. Matiashvili, A.C. Fraser-Smith and A. Bernardi (1992). Results of ULF magnetic field measurements near the epicenters of the Spitak (Ms=6.9) and Loma Prieta (Ms=7.1) earthquakes: comparative analysis, Geophys. Res. Lett., 19, 1495-1498.

Molchanov, O.A., and M. Hayakawa (1995). Generation of ULF electromagnetic emissions by microfracturing, Geophys. Res. Lett., 22, 3091-3094.

Molchanov, O.A., and M. Hayakawa (2008). Seismo-Electromagnetics and Related Phenomena: History and Latest Results, TERRAPUB, Tokyo.

Nagao, T., Y. Orihara, T. Yamaguchi, I. Takahashi, K. Hattori, Y. Noda, K. Sayanagi and S. Uyeda (2000). Co-seismic geoelectric potential changes observed in Japan, Geophys. Res. Letters, 27, 1535-1538.

Parks, G.A. (1965). The isoelectric points of solid oxides, solid hydroxides, and aqueous hydroxo complex systems, Chem. Rev., 65, 177-198.

Pilipenko, V., and E. Fedorov (2014). Coupling mechanism between geoacoustic emission and electromagnetic anomalies prior to earthquakes, Research in Geophysics, 4:5008; doi:10.4081/rg.2014.5008.

Pride, S. (1994). Governing equations for the coupled electromagnetics and acoustics of porous media, Phys. Rev. B 50, 15678-15696.

Sparnaay, M.J. (1972). The electrical double layer (vol. 4 of Properties of Interfaces; Topic 14 of The International Encyclopedia of Physical Chemistry and Chemical Physics), Pergamon Press, Oxford.

Surkov, V.V. (1997). The nature of electromagnetic forerunners of earthquakes, Transactions of the Russian Academy of Science, Earth Science Sections, 355, 945-947.

Surkov, V.V., and V.A. Pilipenko (1997). Magnetic effects

due to earthquakes and explosions: a review, Annali di Geofisica, 40, 227-239.

Surkov, V.V., and V.A. Pilipenko (1999). The physics of pre-seismic electromagnetic ULF signals, In: M. Hayakawa (ed.), Atmospheric and Ionospheric Phenomena Associated with Earthquakes, TERRAPUB, Tokyo, 357-370.

Surkov, V.V., S. Uyeda, H. Tanaka and M. Hayakawa (2002). Fractal properties of medium and seismo-electric phenomena, J. Geodyn., 33, 477-487.

Surkov, V.V., and M. Hayakawa (2006). ULF geomagnetic perturbations due to seismic noise produced by rock fracture and crack formation treated as a stochastic process, Phys. Chem. Earth, 31, 273-280.

Surkov, V.V., and M. Hayakawa (2014). Ultra and Extremely Low Frequency Electromagnetic Fields, Springer Geophysics.

Thomas, J.N., J.J. Love and M.J.S. Johnston (2009). On the reported magnetic precursor of the 1989 Loma Prieta earthquake, Phys. Earth Planet. In., 173, 207-215.

Tzanis, A., and F. Vallianatos (2002). A physical model of electrical earthquake precursors due to crack propagation and the motion of charged edge dislocations, In: M. Hayakawa and O. Molchanov (eds.), Seismo Electromagnetics: Lithosphere - Atmosphere - Ionosphere Coupling, TERRAPUB, Tokyo, 117-130.

Uyeda, S., M. Hayakawa, T. Nagao, O.A. Molchanov, K. Hattori, Y. Orihara, K. Gotoh, Y. Akinaga and H. Tanaka (2002). Electric and magnetic phenomena observed before the volcano-seismic activity in 2000 in the Izu islands regions, Japan, Proc. Natl. Acad. Sci. USA, 99, 7352-7355.

Vallianatos, F., A. Nardi, R. Carluccio and M. Chiappini (2012). Experimental evidence of a non-extensive statistical physics behavior of electromagnetic signals emitted from rocks under stress up to fracture. Preliminary results, Acta Geophys., 60, 894-909.

Zlotnicki, J. and Y. Nishida (2003). Review of morphological insights of self-potential anomalies on volcano, Surv. Geophys., 24, 291-338.

---

*Corresponding author: Vadim V. Surkov,
National Research Nuclear University MEPhI, Moscow, Russia;
email: surkovvadim@yandex.ru.

Appendix A: EK current through a channel with elliptic cross-section

To perform integration in Equation (4) we first introduce the elliptic coordinates μ and ν according to $x = c\cosh\mu\cos\nu$, $y = c\sinh\mu\sin\nu$, where $\mu \geq 0$, $0 \leq \nu < 2\pi$ and $c^2 = a^2 - b^2 (a > b)$. The lines $\mu(x,y) = C_1$ and $\nu(x,y) = C_2$ (C_1 and C_2 are constants) determine the families of confocal ellipses and hyperboles which form an orthogonal grid. Taking the notice of Lame coefficients $h_\mu = h_\nu = c(\sinh^2\mu + \sin^2\nu)^{1/2}$, the unit cross-section is $dS = h_\mu^2 d\mu d\nu$. The Laplace equation for the potential φ is given by

$$\nabla^2\varphi = h_\mu^{-2}\left(\frac{\partial^2\varphi}{\partial\mu^2} + \frac{\partial^2\varphi}{\partial\nu^2}\right) \qquad (A1)$$

Since inside the EDL the electric potential φ varies most rapidly along the direction normal to the wall, the derivative with respect to ν in Equation (A1) can be neglected. Taking into account this approximation and substituting Equations (1) and (A1) into Equation (4) we get:

$$\langle \mathbf{j}_{EK}\rangle = \frac{ab\varepsilon\varepsilon_0\nabla P}{2\pi\eta\left(a^2+b^2\right)}\int\limits_0^{2\pi}d\nu\int\limits_0^{\mu_{max}}\left[1-c^2\left(\frac{\cosh^2\mu\cos^2\nu}{a^2}+\right.\right.$$
$$\left.\left.+\frac{\sinh^2\mu\sin^2\nu}{b^2}\right)\right]\frac{\partial^2\varphi}{\partial\mu^2}d\mu \qquad (A2)$$

Integrating Equation (A2) by parts and taking into account that $\cosh\mu_{max} = a/c$, $\sinh\mu_{max} = b/c$, and $\delta\varphi(0)/\delta\mu = 0$, we come to

$$\langle \mathbf{j}_{EK}\rangle = \frac{abc^2\varepsilon\varepsilon_0\nabla P}{2\pi\eta\left(a^2+b^2\right)}\int\limits_0^{2\pi}\left(\frac{\cos^2\nu}{a^2}+\right.$$
$$\left.+\frac{\sin^2\nu}{b^2}\right)d\nu\int\limits_0^{\mu_{max}}\sinh 2\mu\frac{\partial\varphi}{\partial\mu}d\mu \qquad (A3)$$

Considering the fact that φ changes rapidly in the narrow EDL near the walls and $\delta\varphi/\delta\mu$ tends to zero as $\mu \to 0$, we set $\mu = \mu_{max}$ in the factor $\sinh 2\mu$ in the integrand. We can thus perform the integration in Equation (A3), arriving at

$$\langle \mathbf{j}_{EK}\rangle = \frac{\varepsilon\varepsilon_0\nabla P}{\pi\eta\left(a^2+b^2\right)}\int\limits_0^{2\pi}\left(a^2\sin^2\nu+\right.$$
$$\left.+b^2\cos^2\nu\right)\left[\varphi(\mu_{max})-\varphi(0)\right]d\nu \qquad (A4)$$

Assuming that $\zeta = \varphi(\mu_{max}) - \varphi(0)$ is a constant value and performing integration in Equation (A4), we arrive at Equation (5).